

Quantum Confined One-Dimensional Electron-Hole Plasma in Semiconductor Quantum Wires

R. Cingolani,^(a) H. Lage, L. Tapfer,^(b) H. Kalt, D. Heitmann, and K. Ploog

Max-Planck-Institut für Festkörperforschung, Heisenbergstrasse 1, D-7000 Stuttgart 80, Federal Republic of Germany
(Received 5 June 1991)

We report a study of the temporal evolution of the luminescence from an electron-hole plasma confined in GaAs quantum wires under high-power excitation. In the spectra 1D intersubband transitions with quantum numbers as high as $n=5$ are resolved. The spectral positions are in excellent agreement with Kohn-Luttinger calculations based on an active wire width of $w=60\pm 5$ nm, accurately determined by an x-ray-diffraction method employed for 1D systems. The decay of the luminescence and the hot-carrier cooling rate, which is obtained from line-shape analysis, are found to be slower than the corresponding processes in quantum wells.

PACS numbers: 73.20.Dx, 73.40.Kp, 78.55.Cr, 78.70.Ck

In recent years the study of low-dimensional systems has attracted much attention. These systems are usually fabricated by an ultrafine patterning of layered semiconductor systems. Unipolar one-dimensional electron systems (1DES) and 0DES have been studied in modulation-doped quantum wires and dots. The optical properties of undoped quantum wires are strongly governed by 1D excitonic effects [1-5]. Here we present the first study of a quantum confined 1D electron-hole plasma excited by high-power laser pulses and the investigation of the time dynamics of the radiative recombination processes occurring in the dense electron-hole plasma (EHP) confined in an array of semiconductor quantum-well wires (QWW). A suitable design of the GaAs/ $\text{Al}_{0.36}\text{Ga}_{0.64}\text{As}$ heterostructure configuration allows us to clearly observe the luminescence of 1D intersubband transitions with quantum numbers as high as $n=5$. The separation of the higher-energy transitions agrees well with the calculated confinement energies adopting the structural parameters determined by a suitable x-ray-diffraction technique, employed for the study of 1D structures. A decay time of the order of 800 ps is measured for the electron-hole plasma luminescence, indicating a slower carrier cooling rate as compared to semiconductor quantum wells.

The investigated samples are realized by microstructuring a GaAs/ $\text{Al}_{0.36}\text{Ga}_{0.64}\text{As}$ multiple-quantum-well heterostructure consisting of 25 wells of 10.6-nm width sandwiched among 15.3-nm-wide barriers grown by molecular-beam epitaxy (MBE). The key feature of the investigated structure is that the quantum wells are grown on top of a 1- μm -thick $\text{Al}_{0.36}\text{Ga}_{0.64}\text{As}$ cladding layer. This provides an efficient optical confinement of the luminescence due to the refractive index discontinuity at the interface of about 7% resulting in a considerable increase of the spontaneous luminescence efficiency and in a lowering by about 1 order of magnitude of the stimulated emission threshold at room temperature [6]. The quantum wires have been prepared starting from holographically defined arrays of periodic photoresist stripes acting as masks for a dry mesa-etching process [7].

For the explanation of the optical data it is very important to determine the actual structural parameters of the quantum wire array. This has been performed by employing a suitable experimental and theoretical method based on x-ray-diffraction experiments for 1D systems [8]. Bragg diffraction measurements were performed in symmetric (400) and (200) as well as asymmetric (422) reflection geometry. The asymmetrical (422) reflection was recorded with $\gamma_0 < \gamma_h$ and $\gamma_0 > \gamma_h$, where $\gamma_0 = \sin\theta_i$ and $\gamma_h = \sin\theta_e$ are the direction cosines [9]. The azimuth angle for each reflection measurement was chosen in order to be either sensitive or insensitive to the quantum wire structure, i.e., with the quantum wires perpendicular (y axis) and parallel (x axis) to the scattering plane, respectively. Figure 1 shows the (422) diffraction pattern

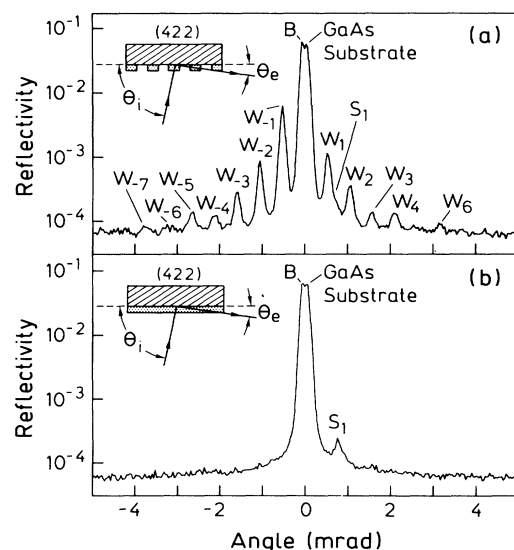


FIG. 1. Asymmetric (422) x-ray-diffraction pattern with the quantum wire structure (a) perpendicular and (b) parallel to the scattering plane. The satellite peaks in (a) are produced by the periodic array of the quantum wires along the (100) surface.

recorded in the $\gamma_0 > \gamma_h$ configuration, which is the most sensitive reflection geometry for the observation of quantum wire structures. In Fig. 1(a) the QWWs are perpendicular to the scattering plane. The satellite peaks of the m th order (labeled W_m), which arise from the periodic wire structure, are well pronounced. On the other hand, no peaks from the quantum wire structure can be observed in the (422) diffraction pattern of Fig. 1(b) recorded with the QWWs parallel to the scattering plane. The satellite peak (S_1) must be attributed to the quantum-well structure, i.e., to the superperiodicity normal to the sample surface. In Fig. 1(a) the angular distance between two satellite peaks of order m and n ($\omega_{m,n}$) is related to the quantum wire period L_p by the equation

$$L_p = \frac{\lambda |\gamma_0| |m - n|}{\sin 2\theta_B \omega_{m,n}}, \quad (1)$$

where λ is the x-ray wavelength ($\lambda_{\text{CuK}\alpha_1} = 1.5404562 \text{ \AA}$) and θ_B is the kinematic Bragg angle. In addition, the intensity ratio $r(m,n)$ between the satellite peaks of order m and n is a measure of the quantum wire profile $W(y)$ [10],

$$r(m,n) = \left| \frac{\int_0^L W(y) e^{2\pi i m y/L} dy}{\int_0^L W(y) e^{2\pi i n y/L} dy} \right|^2. \quad (2)$$

The quantitative analysis of the experimental spectrum of Fig. 1(a) through Eqs. (1) and (2) gives for the quantum wire period $L_p = 2800 \text{ \AA}$ and for the averaged QWW width $L_y = 60 \pm 5 \text{ nm}$. The uncertainty is mainly due to fluctuations of the wire width, which is most probably varying over the sample. It is worth noting that the geometrical wire width determined by scanning electron micrographs (SEM) on this sample is $W = 140 \text{ nm}$. Since the x-ray-diffraction method is only sensitive to the crystalline part of the wire, we conclude that on either side of the wire a region of width $W_a = (W - L_y)/2 \approx 40 \text{ nm}$ is slightly amorphized, this due to ion channeling and, possibly, to redeposition during the etching process. As we will show in the following, the results of our optical measurements demonstrate that these regions act as nearly perfect (infinitely high) barriers for the electrons and holes, thus confirming that the crystalline wire width $L_y \approx 60 \text{ nm}$ deduced by the x-ray-diffraction experiments is indeed the "active" width. A detailed discussion of the x-ray diffraction in semiconductor quantum wire structures will be published elsewhere [11].

The time-resolved luminescence measurements have been performed by using a high-power frequency-doubled, amplified, actively and passively mode-locked Nd-doped yttrium-aluminum-garnet laser, providing 25-ps pulses at 5-Hz repetition rate. The peak power density obtained after focusing over a spot of about $800 \mu\text{m}$ was about 20 MW cm^{-2} . The luminescence was dispersed by a 25-cm spectrometer followed by a single-shot streak camera with a two-dimensional charge-coupled device

detector. The overall time resolution was about 20 ps.

The strong improvement of the light emission by the optical confinement layer has now been fully exploited to measure the luminescence emitted by a dense electron-hole plasma confined in the wire. In Figs. 2(a) and 2(b) we depict the time-resolved luminescence spectra of the electron-hole plasma confined in the QWW at two different excitation intensities. The spectra clearly exhibit several intersubband transitions involving higher-energy QWW states up to quantum numbers as high as $n=5$. Because of the high photogeneration rates of our experiment a broad emission band can be observed during the first 100 ps after the excitation. During this short transient the dense carrier population fills all the available 1D states and the emission spectrum consists of flat and very broad structures [see Fig. 2(b)]. For delays longer than 150 ps carriers recombine and relax into lower-energy quantum wire subbands, resulting in the appearance of several peaks whose energy position does not vary in time and is almost independent of the excitation intensity. At longer delays ($> 400 \text{ ps}$) the spectra exhibit a few structures around the $n=1$ quantum wire emission. The luminescence decay times range between about 400 ps for the higher-energy transitions to 800 ps for the ground-state luminescence (originating from the recombination of electrons and holes at the $n=1$ conduction and valence 1D subbands) and are found to depend on the carrier density, especially on the high-energy tail of the emission spectrum. This lifetime is longer than the one measured in the quantum-well reference sample un-

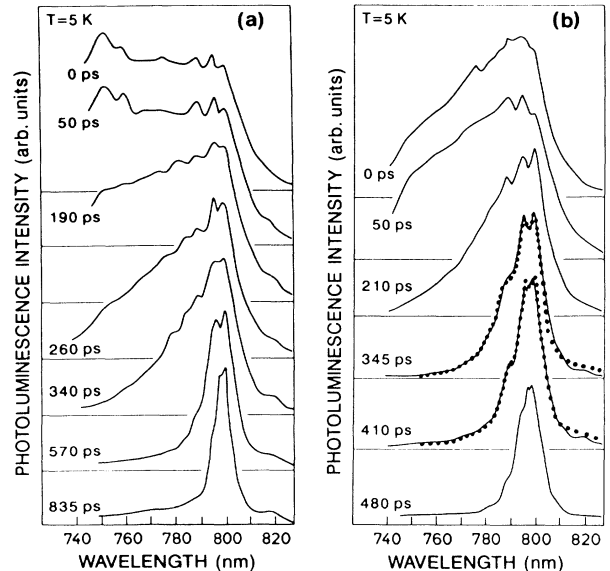


FIG. 2. Time-resolved electron-hole plasma luminescence in quantum wires at 5 K. The excitation intensities for these spectra are $2 \times I_0$ in (a) and I_0 in (b), where I_0 is 0.5 MW cm^{-2} . The dots reproduce the calculated luminescence line shape (see text).

der similar excitation conditions, $\tau \approx 500$ ps [12].

In Fig. 3 we depict the positions of the peaks in the photoluminescence spectra for different decay times. The one-particle carrier confinement energies in QWWs have been calculated by Bockelmann and Bastard [13] in a numerical Kohn-Luttinger-type treatment adopting a square-well model with finite barriers in the z direction and infinite barriers for the y direction (wire-quantization axis). The important point is that the valence-band structure in QWWs has inherently a mixed heavy- and light-hole character, which significantly influences the 1D energy levels. The calculated energy separations of the various 1D intersubband transitions for a well width of 10.6 nm, an *active* wire width of 55 nm, an electron effective mass of $m_e^* = 0.067m_0$, and assuming the $\Delta n = 0$ selection rule, are indicated in Fig. 3 as straight lines. The agreement between the calculated and the experimental data points is excellent. This demonstrates experimentally the importance of the mixing between light- and heavy-hole states in quantum wires. It also strongly supports the results of the x-ray-diffraction measurements which give an active wire width much smaller than the geometrical width observed in the SEM. Further, the successful application of the infinite potential barrier model along the wire quantization direction demonstrates that the amorphized regions of about 40 nm on both sides

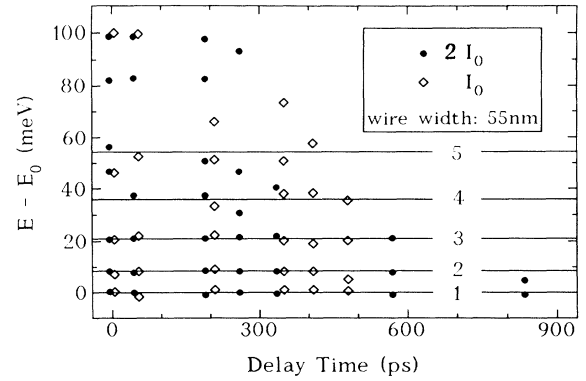


FIG. 3. Comparison between the experimental subband separations taken from the spectra of Figs. 2(a) and 2(b) (symbols) and the calculated differences of quantum wire intersubband transitions with quantum numbers up to $n=5$ (the selection rule $\Delta n=0$ is assumed). E_0 denotes the transition energy between the lowest 1D electron and hole subband.

of the wires act as almost perfect potential barriers.

Information on the ground-level parameters of the EHP confined in the QWW structure are obtained by evaluating the line shape of the electron-hole recombination $R(\hbar\omega)$. We adopt a multisubband momentum-conserving model with constant matrix elements. The band-filling luminescence in this simple case reads

$$R(\hbar\omega) \approx \sum_{i=1}^n f_e(\epsilon_e + E_g^i) [1 - f_h(-\epsilon_h)] \int D_{1D}(E') L(\Gamma, \hbar\omega - E_g^i - E') dE', \quad (3)$$

where the subband index i runs over n occupied subbands, D_{1D} is the 1D density of states broadened by convolution with a Lorentzian function L (Landsberg broadening), and the electron and hole energies are expressed as

$$\epsilon_{e(h)} = \frac{m_{h(e)}}{m_e + m_h} (\hbar\omega - E_g^i) \quad (4)$$

according to k -conservation requirements. Typical calculated spectra adopting the intersubband transition energies E_g^i determined above are shown in Fig. 2(b) superimposed on the experimental curves recorded after delays of 345 and 410 ps. The agreement is good despite the simplifying assumptions made in the model. In the calculations the electron temperature kT , the broadening parameter Γ , and the electron quasi-Fermi level F_e have been used as free parameters. The fit is sensitive to the changes in the total quasi-Fermi level and in the electron temperature which affect the bandwidth and the broadening of the high-energy tail of the luminescence spectra, respectively, and the filling of higher-energy subbands. The broadening parameter in the density of states mainly affects the low-energy tail of the luminescence without appreciable changes in the overall spectral linewidth. The best fit of the spectra of Figs. 2(a) and 2(b) at different delays provides the time evolution of the carrier temperature. This is shown in Fig. 4 at two different pho-

togeneration rates. The carrier temperature decreases in time from 230 down to 60 K during the first 500 ps (I_0 curve), and strongly depends on the excitation intensity. The comparison of these results with those obtained in

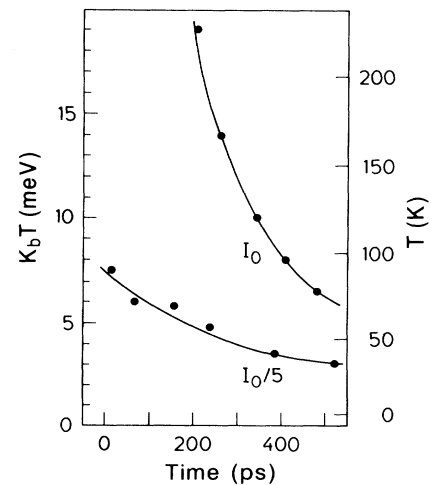


FIG. 4. Time evolution of the carrier temperature obtained from the line-shape fitting of the electron-hole plasma luminescence at two different excitation intensities.

the same manner from the quantum-well reference sample under similar excitation conditions indicates that the hot-carrier cooling rate is slower in QWWs than in quantum wells [14]. This is consistent with the observed longer luminescence decay time of the EHP. It may be also an indication for a reduced phonon scattering rate in the type of 1D structures we have investigated, since the interaction of phonons with carriers depends in 1D systems on the structural parameters [15]. A systematic study of the carrier temperature as a function of time and carrier density is in progress and will be the subject of a forthcoming paper.

In conclusion, we have investigated the temporal evolution of the electron-hole plasma luminescence in GaAs quantum wires. The use of a high optical confinement heterostructure allows us to observe radiative recombination from high-index intersubband transitions up to $n=5$ in the wire. The active width of the crystalline part of the QWW determined by a suitable technique based on x-ray diffraction is found to be considerably smaller than the geometrical wire width observed by scanning electron micrographs. This active wire width has been employed in the calculation of the 1D confinement energies. Excellent agreement is found between the observed luminescence spectra and the 1D intersubband transition energies calculated taking into account the valence subband dispersion and assuming a simple infinite square-well potential model along the wire quantization axis [13]. The time-resolved luminescence shows an electron-hole plasma decay time of about 800 ps. Further, a momentum conserving, multisubband electron-hole recombination model has been used to calculate the line profile of the electron-hole plasma luminescence spectra at different delays. The hot-carrier temperature indicates a reduced carrier cooling rate in these quasi-one-dimensional systems.

We gratefully acknowledge useful discussions with G. C. LaRocca, P. Lugli, and E. Molinari. We also like to thank A. Fischer for the MBE growth of the excellent

multiple quantum well and C. Lange for the high-quality scanning electron micrographs. This work has been sponsored by the Bundesministerium für Forschung und Technologie of the Federal Republic of Germany.

^(a)Present address: Dipartimento di Scienze dei Materiali, Università di Lecce, Via per Arnesano, 73100 Lecce, Italy.

^(b)Present address: Centro Nazionale Ricerca e Sviluppo dei Materiali, Via G. Marconi 147, 72023 Mesagne (Br), Italy.

- [1] Y. Hirayama, S. Tarucha, Y. Suzuki, and H. Okamoto, *Phys. Rev. B* **37**, 2774 (1988).
- [2] M. Tsuchiya, J. M. Gaines, R. H. Yan, R. J. Simes, P. O. Holtz, L. A. Coldren, and P. M. Petroff, *Phys. Rev. Lett.* **62**, 466 (1989).
- [3] M. Kohl, D. Heitmann, P. Grambow, and K. Ploog, *Phys. Rev. Lett.* **63**, 2124 (1989).
- [4] D. Ghersoni, J. S. Weiner, S. N. G. Chu, G. A. Baraff, J. M. Vandenberg, L. N. Pfeiffer, K. West, R. A. Logan, and T. Tanbunek, *Phys. Rev. Lett.* **65**, 1631 (1990).
- [5] For more references, see K. Kash, *J. Lumin.* **46**, 69–82 (1990).
- [6] R. Cingolani, K. Ploog, A. Cingolani, C. Moro, and M. Ferrara, *Phys. Rev. B* **42**, 2893 (1990).
- [7] P. Grambow, E. Vasiliadou, T. Demel, K. Kern, D. Heitmann, and K. Ploog, *Microelectron. Eng.* **11**, 47 (1990).
- [8] L. Tapfer and P. Grambow, *Appl. Phys.* **50**, 3 (1990).
- [9] L. Tapfer and K. Ploog, *Phys. Rev. B* **33**, 5565 (1986).
- [10] A. T. Macrander and S. E. G. Slusky, *Appl. Phys. Lett.* **56**, 443 (1990).
- [11] L. Tapfer *et al.* (to be published).
- [12] R. Cingolani, H. Kalt, and K. Ploog, *Phys. Rev. B* **42**, 7655 (1990).
- [13] U. Bockelmann and G. Bastard, *Europhys. Lett.* **15**, 215 (1991).
- [14] K. Leo, W. W. Ruühle, and K. Ploog, *Phys. Rev. B* **38**, 1947 (1988).
- [15] U. Bockelmann and B. Bastard, *Phys. Rev. B* **42**, 8947 (1990).